

Type Ia Supernova Delay Times and Rates for Double-detonation Sub-Chandrasekhar Mass Models

A.J. Ruiter,^{1*} K. Belczynski,^{2,3} S.A. Sim,^{1,4} W. Hillebrandt,¹ C.L. Fryer,⁵ M. Fink,¹ and M. Kromer¹

¹ *Max Planck Institute for Astrophysics, Karl-Schwarzschild-Str. 1, 85741 Garching, Germany*

² *Astronomical Observatory, University of Warsaw, Al. Ujazdowskie 4, 00-478 Warsaw, Poland*

³ *Center for Gravitational Wave Astronomy, University of Texas at Brownsville, Brownsville, TX 78520, USA*

⁴ *Research School of Astronomy and Astrophysics, Mount Stromlo Observatory, Cotter Road, Weston Creek, ACT 2611, Australia*

⁵ *Los Alamos National Laboratory, CCS-2, MS D409, Los Alamos, NM 87545 USA*

Accepted 20xx Month xx. Received 20xx Month xx; in original form 20xx Month xx

ABSTRACT

We present theoretical delay time distributions and rates of Type Ia supernovae from formation channels that are thought to lead to SNe Ia, including the double-detonation sub-Chandrasekhar mass model, using the population synthesis binary evolution code `StarTrack`. Though much uncertainty in white dwarf accretion physics still exists, we find that within our standard model, sub-Chandrasekhar mass SNe Ia are able to potentially account for the observed rate of SNe Ia. We find that the delay time distribution of sub-Chandrasekhar mass SNe Ia can be divided into two distinct formation channels: the ‘prompt’ helium-star channel with delay times < 500 Myr (13% of all sub-Chandras), and the ‘delayed’ double white dwarf channel, with delay times $\gtrsim 800$ Myr spanning up to a Hubble time (87%). These encouraging findings coincide with recent observationally-derived delay time distributions which show that a large number of SNe Ia are prompt with delay times < 500 Myr, while a significant fraction have delay times spanning ~ 1 Gyr to a Hubble time.

Key words: binaries: close – stars: evolution – supernovae – white dwarfs.

1 INTRODUCTION

The exact nature of the stars that produce Type Ia supernovae (SNe Ia) – which are believed to be thermonuclear explosions of carbon–oxygen (CO) white dwarfs (WDs) close to the Chandrasekhar mass limit – remains unknown (Branch et al. 1995). The most widely favoured SN Ia progenitor scenarios involve the double degenerate scenario (DDS; Webbink 1984; Iben & Tutukov 1984), and the single degenerate scenario (SDS; Whelan & Iben 1973). In the DDS, the merger of two CO WDs with a total mass exceeding the Chandrasekhar mass limit, $M_{\text{Ch}} \sim 1.4 M_{\odot}$, can lead to explosive carbon burning which causes a SN Ia explosion. In the SDS, a CO white dwarf accretes from a hydrogen-rich stellar companion via stable Roche-Lobe overflow (RLOF) and undergoes hydrogen burning on the surface, enabling the WD to accumulate mass toward M_{Ch}

until carbon is ignited explosively in the centre of the WD leading to a SN Ia. However, in the stable RLOF configuration the companion does not have to be a hydrogen-rich main sequence (MS) or giant-like star, but can be a non- or semi-degenerate helium-burning star, or a (degenerate) helium white dwarf (e.g., Iben et al. 1987; Yoon & Langer 2003; Solheim & Yungelson 2005). Like the SDS, the WD explodes once it approaches M_{Ch} (this helium-rich donor scenario, hereafter HeRS, will be discussed further in section 2.3).

Recently, Ruiter et al. 2009 (Paper I) carried out a population synthesis study showing rates and delay times – time from birth of a progenitor system in a short burst of star formation to SN – for three formation channels of SNe Ia: DDS, SDS and HeRS. Here, we extend our study of progenitors and focus our analysis and discussion on the sub- M_{Ch} “double-detonation” model. This scenario, in which a CO WDs accretes from a helium-rich companion filling its Roche-Lobe and explodes as a SN Ia before reaching the M_{Ch} limit, has thus far been regarded as an unlikely model for SNe Ia owing to the fact that most synthetic light curves and spectra of these objects from previous studies did not

* E-mail: ajr@mpa-garching.mpg.de; kbelczyn@nmsu.edu; ssim@mso.anu.edu.au; wfh@mpa-garching.mpg.de; fryer@lanl.gov; mfink@mpa-garching.mpg.de; mkromer@mpa-garching.mpg.de

match those observed for SNe Ia. However, it has recently been argued that the model might be capable of producing a better match to observation, depending on details regarding the manner in which the accreted helium burns (e.g. Fink et al. 2010; Kromer et al. 2010). In either case, the explosion mechanism is expected to produce events that are bright and should be detectable. Thus, quantification of their predicted rates and delay times is an important step for testing our population synthesis models, and for determining what fraction of SNe Ia could conceivably be associated with this channel.

Since these calculations are based on the work that was performed for Paper I, the reader is referred to that paper for a more detailed description of the DDS, SDS and HeRS scenario. The layout of this paper is as follows: In section 2 we summarise some background information on SN Ia progenitors from the literature. In section 3 we discuss the population synthesis modelling. In section 4 we present initial ZAMS mass distributions for the four evolutionary channels, delay time distributions and rates as a function of stellar mass as well as distributions showing the exploding CO WD core mass. In section 5 we close with a discussion of these findings and possible implications/predictions for SN progenitors and their host stellar populations.

2 BACKGROUND

2.1 Recent observations of SNe Ia delay times

The idea that SN Ia progenitors belong to at least two distinct populations (Scannapieco & Bildsten 2005; Mannucci et al. 2006; Pritchett et al. 2008) has recently been gaining ground. Based on further observations, a picture is emerging which supports populations of both quickly-evolving (prompt) progenitors with short delay times less than ~ 500 Myr, as well as more slowly-evolving progenitors with (sometimes rather) long delay times spanning up to a Hubble time (but see also Greggio 2010).

The delay time distribution (DTD) is a useful tool in determining the age of the progenitor stellar population, which places strong constraints on the different proposed progenitor scenarios. There are a growing number of observationally-derived DTDs presented in the literature from various groups (see section 1 of Maoz & Badenes 2010, for an overview of these previous studies). In some studies there are simply not enough data to warrant a thoroughly robust analysis over all possible delay times, and thus far there is no consensus among all of the delay time studies regarding the DTD of SNe Ia.

Mannucci et al. (2006) proposed that 50% of SNe Ia consist of ‘prompt’ progenitors with delay times $\lesssim 100$ Myr, the rest having very long delay times, possibly spanning up to a Hubble time. Raskin et al. (2009), who used the spatial location of SNe Ia in their local environments to derive delay times, found evidence for a prompt component with delay times of 200–500 Myr. It was found by Maoz & Badenes (2010) that a substantial fraction of SNe Ia in the Magellanic Clouds have delay times less than 1 Gyr.¹ They found

that among ‘prompt’ SNe Ia (35–330 Myr delay times in that study) the SN Ia rate² is ~ 0.09 – 0.40 SNum, compatible with the results of Li et al. (2010a), whereas ‘delayed’ events (330 Myr–14 Gyr delay times) had an overall smaller rate: < 0.0024 SNum. This study confirmed that for their sample, roughly half (or more) of SNe Ia occur with delay times $\lesssim 330$ Myr, thus giving further support for a prompt component of the DTD. Maoz et al. (2010b) reconstructed the star formation histories for a sample of LOSS SN host galaxies and found strong evidence for both a prompt Ia component with delay times < 420 Myr and a delayed component with long delay times (> 2.4 Gyr). Brandt et al. (2010) used SN light-curves and spectra from host galaxies of 101 SNe Ia with $z < 0.3$ to construct the DTD, and arrived at a similar conclusion: that roughly half of SNe Ia occur with delay times < 400 Myr, while roughly the other half have long (> 2.4 Gyr) delay times. Further, they find that the short delay time events are more luminous with slowly-declining light-curves, and are associated with young stellar populations, whereas the SNe with long delay times are typically fast-declining, sub-luminous events. Totani et al. (2008) derived the DTD from a large population of old galaxies which only probed delay times $\gtrsim 100$ Myr, and they found that the DTD follows a relatively smooth power-law distribution (t^{-1}) from ~ 0.1 to 8 Gyr.

2.2 Two progenitor scenarios: DDS and SDS

For some time, population synthesis calculations (Iben & Tutukov 1984; Yungelson et al. 1994; Yungelson & Tutukov 1997; Yungelson & Livio 1998; Nelemans et al. 2001; Ruiter et al. 2009) have predicted that the number of merging CO WDs with a total mass exceeding M_{Ch} (DDS) is sufficient to match, and thus possibly account for, the rate of SNe Ia (0.4 ± 0.2 per century for the Galaxy, Cappellaro et al. 1999). At the same time, the theoretically-predicted SN Ia rate from the SDS channel is usually unable to explain the observed rates of SNe Ia (see also Gilfanov & Bogdán 2010). An exception is the study by Meng & Yang (2010), who found that the SDS scenario could account for a Galactic SN Ia rate of $\sim (2.25 - 2.6) \times 10^{-3}$ per year. Meng & Yang (2010) adopt the ‘strong mass stripping effect’ of Hachisu et al. (2008) for hydrogen-rich donors, as well as a thermally-unstable disc model, the latter which enables a larger number of SDS progenitors to pass through the parameter space in which a SN Ia is assumed to take place in that study. The strong mass stripping effect alone is unlikely to account for the majority of SNe Ia, since the model predicts a hydrogen-rich torus surrounding the WD, and if not fully dispersed at the time of explosion, might leave behind observational signatures (in particular for giant donors, Hayden et al.

85% of SNe Ia explode within the first Gyr of star formation, and the DTD is well-fit by a power-law of $t^{-1.2}$ for delay times > 400 Myr.

² The supernova rate in the local Universe as a function of Hubble type was recently presented in the study of Li et al. (2010a). They found the SN Ia rate to be constant across galaxy Hubble type (when upper limits set by irregular galaxies were neglected) with a value of 0.136 ± 0.018 SNum (1 SNum = SNe Ia per century per $10^{10} M_{\odot}$).

¹ A complimentary result was also determined by Maoz et al. (2010a), who found that in galaxy clusters out to $z = 1.45$ 50-

2010). There are very few SNe Ia that show hydrogen lines in their spectra; if the progenitor involved a hydrogen-rich companion, one may expect H α to be detectable in the nebular spectra more frequently (Leonard 2007).

Han & Podsiadlowski (2004) found a SDS Galactic rate of $(0.6 - 1.1) \times 10^{-3}$ SNe Ia per year, which is only a factor of a few below the observationally-inferred rate. However it must be noted that in Han & Podsiadlowski (2004), as mentioned in that work, the accretion prescription is adopted from Hachisu et al. (1999), which utilises an efficiency for hydrogen accretion that is somewhat optimistic, in contrast to the narrower range of accretion rates which is found to give rise to stable hydrogen burning in other studies of nuclear burning on WDs (Priyalnik & Kovetz 1995; Nomoto et al. 2007; Shen & Bildsten 2007).

The DDS is an attractive model for SNe Ia, given the theoretically predicted occurrence rate as well as the fact that CO WD mergers are systems that are essentially devoid of hydrogen. The main argument against the DDS is that detailed WD merger calculations indicate that the merging process leads to physical conditions in which a thermonuclear explosion is unlikely (Yoon et al. 2007). It is more probable that a merger between two CO WDs with a total mass $>M_{\text{Ch}}$ will collapse and form a neutron star; an accretion induced collapse (AIC, Miyaji et al. 1980; Saio & Nomoto 1985; Nomoto & Kondo 1991, and references therein)³. Based on modern collapse calculations (Fryer et al. 1999; Dessart et al. 2007; Abdikamalov et al. 2010), Fryer et al. (2009) found that these AICs produced outbursts that were $\sim 1-3$ magnitudes dimmer than typical SNe Ia, arguing that AICs could only explain a few abnormal Ia explosions.

In a merger of two CO WDs, once the larger (less massive) WD fills its Roche-lobe, it is likely to be disrupted and rapidly accreted by the companion. This process can be quite violent, and might under the right conditions lead to a SN Ia explosion (Piersanti et al. 2003). For example, in the DDS case involving the merger of two WDs with a mass ratio close to unity, where the WDs each have a mass $\sim 0.9 M_{\odot}$ (Pakmor et al. 2010a), critical conditions for the successful initiation of a detonation (Seitenzahl et al. 2009) can be obtained. The Pakmor et al. (2010a) study found that these DDS systems can both in number and in observational characteristics account for the population of sub-luminous 1991bg-like SNe Ia. However, the 1991bg-like systems only account for *at most* 18% (Li et al. 2010b) of SNe Ia.

For lower mass ratios (see Pakmor et al. 2010a, Pakmor et al. 2010b, in prep.) it is unlikely that the merger would lead to a SN Ia as the achieved densities are not high enough to enable a detonation to occur. In such WD mergers, high accretion rates onto the relatively ‘cold’ primary WD can lead to carbon burning off-centre, where the densities are too low, and carbon does not burn explosively. The primary CO WD will in turn burn carbon and evolve into an oxygen–neon–magnesium (ONeMg) WD (Nomoto & Kondo

1991). As the ONeMg WD increases in mass, density and temperature conditions become more favourable for electron captures, which in turn remove electron degeneracy pressure from the undisrupted WD. As the WD approaches M_{Ch} , the central densities continue to increase and the WD collapses to become a neutron star before a thermonuclear explosion can take place.

In population synthesis calculations, it is typically assumed that all mergers of CO–CO WDs produce a SN Ia provided that the total mass exceeds M_{Ch} . If some (or many) of these CO–CO mergers result in AIC then the observed SN Ia rates cannot be fully explained by the DDS model. Thus, if it is true that the majority of the DDS systems cannot produce events that look like SNe Ia, and there are not enough SDS or HeRS events, then a significant fraction of SNe Ia remain to be accounted for.

2.3 The helium donor formation channels

2.3.1 Chandrasekhar mass explosions

We delineate between the SDS and HeRS since the latter can involve either one degenerate star where the donor is helium-burning, or two, where the donor is a helium-rich WD. Double WDs will have very close orbits (orbital periods < 70 minutes) as is the case for typical AM CVn binaries (see Nelemans et al. 2001, 2010, for a discussion on AM CVn stars). In Paper I the rates and delay times from three formation channels involving exploding WDs with masses $\geq M_{\text{Ch}}$ (DDS, SDS and HeRS) were investigated. Both helium-donor channels were referred to as the ‘AM CVn channel’ in Paper I. However, it is possible that in the case of an evolved helium star donor, the orbital separation can be rather large, and thus labelling such a system as an AM CVn binary is perhaps not appropriate. Thus in this paper we adopt the acronym HeRS for all SN Ia progenitors in which the Chandrasekhar mass WD explodes once it has accreted sufficient mass in stable RLOF from a helium-rich companion, whether the donor is degenerate or non-degenerate. This scenario includes AM CVn binaries as well as WDs accreting from helium-burning stars; including those which are evolved.

SN Ia rates of the HeRS scenario leading to SNe Ia have been previously investigated by different groups: Solheim & Yungelson (2005); Ruiter et al. (2009); Wang et al. (2009a,b); Meng & Yang (2010), some of whom considered only the helium-burning star channel. In the majority of studies it was found that the HeRS is unable to account for the rates of SNe Ia.⁴ In many cases, theoretically-motivated studies of the HeRS channel produce SNe Ia with short delay times ($\lesssim 10^8$ Myr), and are not able to account for a large number of systems at long delay times.

³ AIC events may also occur when a massive (e.g., oxygen–neon–magnesium) WD accretes via RLOF from a stellar companion approaching $\sim 1.38 M_{\odot}$. Henceforth we will refer to this RLOF AIC formation channel as the ‘RLOF AIC’, and the double degenerate massive WD merger channel as the ‘merger AIC’.

⁴ Wang et al. (2009a) found Galactic SN Ia rates which were higher than the other studies: $\sim 10^{-3} \text{ yr}^{-1}$. However this rate is likely somewhat optimistic, since in that study they consider a rather large range of orbital periods at the moment of RLOF onset between the WD and the helium star (up to > 100 days for the most massive WD accretors).

2.3.2 *sub-Chandrasekhar mass explosions*

Thermonuclear explosions may occur in systems with a sub- M_{Ch} (probably CO) WD accreting via stable RLOF from a helium-rich companion (Iben & Tutukov 1991; Yungelson & Livio 2000). It has been shown that at certain (low) accretion rates on to the WD helium flashes on the WD surface are inhibited (Kawai et al. 1987; Ivanova & Taam 2004), and the WD can steadily and efficiently build up a massive layer of helium on the surface. In such a massive degenerate helium shell (e.g., $\sim 0.1 M_{\odot}$ of helium, Taam 1980), a flash may likely evolve as a violent detonation, which may also trigger a detonation of the CO core, and thus a thermonuclear explosion of the complete star (e.g., Livne 1990; Woosley & Weaver 1994; Livne & Arnett 1995).⁵

Sub- M_{Ch} models of SNe Ia are appealing for a number of reasons. Population synthesis calculations have already shown that the DTD for the double-detonation sub- M_{Ch} explosion model (sometimes referred to as edge-lit detonation, ELD; see Yungelson & Livio 2000, and references therein) spans a wide range at early times. Yungelson & Livio (2000) investigated the double-detonation scenario for helium star and hydrogen-rich donors, and found a corresponding delay time of $\sim 30 \text{ Myr} - 1.3 \text{ Gyr}$ for the helium star donor systems. Also, population synthesis modelling has indicated that the number of potential progenitors for the double-detonation sub- M_{Ch} SNe Ia involving helium-rich donors alone may be large enough to account for the observed rates (e.g., Tout et al. 2001; Regös et al. 2003; Ruiter et al. 2009). Additionally, simplistic studies of pure detonations of sub- M_{Ch} WDs (in the absence of any overlying helium shell) indicate that the synthetic light curves and spectra from sub- M_{Ch} explosions may be able to reproduce a surprising number of the observed properties of SNe Ia (Sim et al. 2010), and even variations within the class that could be associated with differences in the mass of the exploding WD.

The Sim et al. (2010) work, however, neglects the issue of how the outer helium layer will affect the observables. Several previous studies have calculated detailed synthetic light-curves and spectra of sub- M_{Ch} double-detonation models (e.g. Hoefflich & Khokhlov 1996; Nugent et al. 1997). These concluded that such explosions would likely not lead to events with observational properties characteristic of normal SNe Ia. In general, the light curves were found to rise and fall too rapidly compared to ‘normal’ SNe Ia while their spectra were too blue to match sub-luminous SNe Ia and lacked sufficiently strong features of intermediate mass elements, such as Si and S. Importantly, most of these discrepancies with observation can be traced to the presence of the products of helium burning (^{56}Ni and other iron-group elements) in the

outer regions of the ejecta, and those studies mainly considered systems in which a relatively massive ($\sim 0.2 M_{\odot}$) helium layer had accumulated on the WD ($\sim 0.6 M_{\odot}$) surface. More recently, Bildsten et al. (2007) and Shen & Bildsten (2009) have shown that conditions suitable for detonation in the WD might be reached for somewhat lower helium shell masses than considered in most previous studies: perhaps as low as $0.05 M_{\odot}$ for a CO WD (core) mass of $1.0 M_{\odot}$ (in general the more massive the CO WD, the less massive the accumulated helium layer needs to be for a detonation). Fink et al. (2010) have shown that, even for such low helium shell masses, detonation of the helium will robustly lead to an explosion of the underlying WD. With a significantly lower He shell mass (and thus fewer iron-group elements in the outer ejecta), this may open the door for double-detonation sub- M_{Ch} models whose spectra and light curves are in better agreement with observed SNe Ia. This has been investigated by Kromer et al. (2010) who computed synthetic observables for the Fink et al. (2010) simulations. They showed that even very low mass ($0.05 M_{\odot}$) helium shells affect the observable display and can lead to spectroscopic signatures that are not characteristic of observed SNe Ia. However, Kromer et al. (2010) also highlighted that the results are highly sensitive to the details of the nucleosynthesis that occur during burning of the helium shell. Modifications to the burning – as might be achieved by considering a composition other than pure helium – could allow the model predictions to achieve much better agreement with observation.

Taken together, the body of theoretical work strongly suggests that the sub- M_{Ch} double-detonation scenario is physically realistic. Depending on the details of the accumulated helium layer and its burning products, the explosion may closely resemble observed “normal” SNe Ia or it might be highly spectroscopically peculiar – but regardless of this, it certainly can be bright enough to be readily observable – for a CO WD of around $1.0 M_{\odot}$ the luminosity produced following detonation is expected to be close to that of a normal SN Ia (Shigeyama et al. 1992; Sim et al. 2010). Given that potential progenitors are also expected to be common, we are therefore compelled to further investigate this progenitor scenario. If these explosions can produce events that resemble “normal” SNe Ia then it is of interest to quantify the fraction of observed SNe Ia that might be accounted for via this channel. Alternatively, if these explosions are realised in nature but are spectroscopically peculiar, it is important to estimate their predicted rate and consider whether the apparent lack of observational detections is a major concern for the established theory; the lack of such events may challenge our understanding of either (or both) the explosion physics or the progenitor binary evolution. For this scenario it is of particular interest to consider the DTD predicted for this class of explosion and to investigate any correlations between the properties of the exploding system (particularly the mass of the primary WD, which likely determines the brightness of the explosion) and the age of the stellar population in which it resides.

⁵ It is possible that the companion can be hydrogen-rich where hydrogen burns steadily on the surface of the WD, building up a helium-rich layer on top of the CO WD which can detonate (Kenyon et al. 1993; Piersanti et al. 1999; Yungelson & Livio 2000). Such a double-detonation scenario for hydrogen-rich donors was investigated by Yungelson et al. (1995), who have shown that sub-Chandrasekhar mass WDs accreting hydrogen in symbiotic binaries may be capable of producing up to $\sim \frac{1}{3}$ of all SNe Ia, provided that accreting WDs with masses as low as $0.6 M_{\odot}$ are able to successfully undergo double-detonations. However in this work, we only consider helium-rich donors as possible companions for double-detonation sub- M_{Ch} SN Ia progenitors.

3 MODEL

It has been shown that a WD accumulating helium-rich material may be capable of exploding as a SN Ia if the correct conditions are satisfied, even if the WD is below M_{Ch} (Taam 1980; Iben et al. 1987; Iben & Tutukov 1991; Woosley & Weaver 1994; Livne & Arnett 1995; Ivanova & Taam 2004). In Belczynski et al. (2005), sub- M_{Ch} models were calculated, though DTDs for different formation channels were not discussed separately, and rates were not presented in that work. In Paper I, rates and delay times were presented only for $\gtrsim M_{\text{Ch}}$ WD mass models where as here, we additionally include sub- M_{Ch} SNe Ia progenitors in our study.

All sub- M_{Ch} SN progenitors in our calculations involve a CO WD accreting via RLOF from a helium-rich companion. As in Paper I, if the donor is a WD then it can be either a helium WD or a hybrid WD; a WD with a CO core and a helium-rich mantle. Hybrid WDs are formed through binary evolution when a red giant is stripped of its envelope through binary interactions, and the helium core, once helium is ignited, cannot fully complete the helium burning phase. In cases where the stripped helium core does not reach the helium-burning phase, a helium WD is formed.

In the following sections we compute and discuss rates and delay times for the aforementioned SN Ia evolutionary models that have been proposed as the most promising formation channels for SNe Ia:

- the DDS
- the SDS
- the HeRS
- the double-detonation sub- M_{Ch} scenario involving helium-rich donors

It is important to keep in mind that, while evolution of close binaries remains an active field of research and discovery, no concrete constraints currently exist for the evolution of mass-transferring binaries, nor for the common envelope (CE) phase (e.g., Yungelson 2008). The CE phase is certainly one of the most poorly understood phenomena in close binary evolution, and a theoretical picture of CE evolution is not yet available. Since there are a limited (though growing) number of observations available to guide our choice of parameters, we present results for three different common envelope realizations which most effectively bracket the uncertainties. For the growth of CO WDs during stable RLOF, as was done in Ruiter et al. (2009) we present the results from our population synthesis model using a detailed WD accretion scheme, which was constructed by adopting various input physics from the literature.

We use the `StarTrack` population synthesis binary evolution code (Belczynski et al. 2008) to evolve our stellar populations employing Monte Carlo methods. The code has undergone many revisions since the first code description publication (Belczynski et al. 2002). Many of the updates concerning accretion on to WDs can be found in Belczynski et al. (2005, 2008), though since then we have incorporated an updated prescription for accretion of hydrogen on WDs (Nomoto et al. 2007). The initial distributions for binary orbital parameters (orbital periods, mass ratios, etc.) are the same as described in Paper I, section 2.

In Paper I, it was assumed that the ejection of the enve-

lope of the mass-losing star during a CE phase came at the expense of removing the orbital energy of the binary, as dictated by the well-known ‘energy-balance’ (or ‘ α -formalism’) equation (Webbink 1984)

$$\frac{G M_{\text{don},i} M_{\text{ej}}}{\lambda R_{\text{don},i}} = \alpha_{\text{CE}} \left(\frac{G M_{\text{don},f} M_{\text{com}}}{2 a_f} - \frac{G M_{\text{don},i} M_{\text{com}}}{2 a_i} \right) \quad (1)$$

where G is the gravitational constant, $M_{\text{don},i}$ is the initial mass of the (giant) donor star just prior to the CE, M_{ej} is the ejected mass (assumed to be the mass of the giant’s envelope), M_{com} is the mass of the companion (assumed to be unchanged during the CE), $M_{\text{don},f}$ is the final mass of the donor once the envelope has been ejected, $R_{\text{don},i}$ is the initial radius of the donor star when it fills its Roche-Lobe, a_i is the initial orbital separation, a_f is the final orbital separation (if a_f is too small to accommodate the Roche-Lobes of the stars, the CE results in a merger), α_{CE} is the efficiency with which the binary orbital energy can unbind the CE, and λ is a parametrization of the structure of the donor star (de Kool 1990); both α_{CE} and λ are fairly uncertain.

For Models 1 and 2 from Paper I, $\alpha_{\text{CE}} \times \lambda$ values of 1 and 0.5 were adopted, respectively. The major difference was that Model 1 (more efficient removal of the CE) resulted in an overall higher number of SNe. In the current paper, we keep all model parameters the same as in Model 1 of Paper I for one model; we refer to this model as Model A1 (standard model). However, in order to explore the sensitivity of the physical mechanism of CE ejection, which is still not understood, we have run two additional sets of models. There has been some recent observational (Zorotovic et al. 2010) as well as theoretical (Passey et al. 2010, in prep.) evidence that the value for α_{CE} lies between 0.2 and 0.3. Additionally, for low-mass stars a value of 0.5 is often adopted for λ (van der Sluys et al. 2006). Thus to best bracket our uncertainties for the energy balance prescription of CE evolution, in a second model we employ a very low CE ejection efficiency: $\alpha_{\text{CE}} = 0.25$ and $\lambda = 0.5$ yielding $\alpha_{\text{CE}} \times \lambda = 0.125$. We refer to this model as Model A.125. In a third model, we assume a different parametrization for the treatment of the CE phase. We employ the ‘ γ ’ prescription for CE evolution (Nelemans & Tout 2005) every time a CE event is encountered in the code. Henceforth we refer to this model as Model G1.5.⁶ For Model G1.5, all physical parameters are identical to Models A1 and A.125, except that when unstable mass transfer is encountered and a CE ensues, the orbital separation of the binary changes not as a consequence of removing gravitational binding energy from the orbit, but linearly as a function of mass loss (and hence angular momentum loss), parametrized by the factor γ :

$$\frac{a_f}{a_i} = \left(1 - \gamma \frac{M_{\text{ej}}}{M_{\text{tot},i}} \right)^2 \frac{M_{\text{tot},f}}{M_{\text{tot},i}} \left(\frac{M_{\text{don},i} M_{\text{com}}}{M_{\text{don},f} M_{\text{com}}} \right)^2 \quad (2)$$

where $M_{\text{tot},i}$ and $M_{\text{tot},f}$ represent the total mass of

⁶ We note here that in Nelemans & Tout (2005), the ‘ γ ’ prescription is only assumed when the companion (the star *not* undergoing mass loss) is an unevolved star. In all other cases, the classical ‘ α ’ prescription was used; this hybrid-prescription was chosen since it best reproduced observations of the population of post-CE binary systems available at that time. In this work however, we stick to either one of two prescriptions for a given case: α CE for Models A1 and A.125, and γ CE for Model G1.5.

the binary before and after CE, respectively. Following Nelemans & Tout (2005), we have chosen $\gamma = 1.5$.⁷

3.1 Sub-Chandrasekhar mass model: Assumptions

We adopt the prescription of Ivanova & Taam (2004), applied to accretion from helium-rich companions only, to determine when a particular binary undergoes a sub- M_{Ch} SN Ia (Belczynski et al. 2008, see section 5.7.2 for equations). In short, we consider three different accretion rate regimes for accumulation of helium-rich material on *all* CO WDs, adopting the input physics for helium accretion on to WDs of Kato & Hachisu (1999, 2004). At high accretion rates ($\sim 10^{-6} M_{\odot} \text{yr}^{-1}$, and for all cases where the WD accretor mass is $< 0.7 M_{\odot}$), helium burning is stable and thus mass accumulation on the WD is fully efficient ($\eta_{\text{acu}} = 1$). At somewhat lower accretion rates helium burning is unstable and the binary enters a helium-flash cycle, thus accumulation is possible but is not fully efficient ($0 < \eta_{\text{acu}} < 1$). In both of these aforementioned accretion regimes, the CO WD is allowed to accrete (and burn) helium, and its total mass may reach M_{Ch} and explode as a SN Ia through the HeRS channel. However, for low accretion rates ($\sim 10^{-8} M_{\odot} \text{yr}^{-1}$), compressional heating at the base of the accreted helium layer plays no significant role, and a layer of unburned helium can be accumulated on the WD surface. Following Ivanova & Taam (2004), we assume that if such a CO WD accumulating helium enters this ‘low’ accretion rate regime and accumulates $0.1 M_{\odot}$ of helium on its surface, a detonation is initiated at the base of the helium shell layer. Consequently, a detonation in the core of the CO WD is presumed to follow, and we assume that a sub- M_{Ch} SN Ia takes place. Only accreting WDs with a *total mass* $\geq 0.9 M_{\odot}$ are considered to lead to potential sub- M_{Ch} SNe Ia in this work, since lower mass cores may not detonate, and if they do they are unlikely to produce enough radioactive nickel and hence will not be visible as SNe Ia (e.g., Sim et al. 2010, table 1). Thus in all future discussions we refer to sub- M_{Ch} systems whose total WD mass (CO core + helium shell) is at least $0.9 M_{\odot}$ at the time of SN Ia unless otherwise noted; for our population synthesis model, this intrinsically implies that all exploding sub- M_{Ch} SNe Ia have CO WD ‘core’ masses $> 0.8 M_{\odot}$. Helium-rich WDs are simply not massive enough, and we assume that ONeMg WDs do not make SNe Ia.

4 RESULTS

Here we present the ZAMS masses, DTD and rates for all of our SN Ia models, as well as CO WD core masses for our sub- M_{Ch} models. Our results are discussed in the following subsections, but here we give a brief outline of our findings:

We have investigated the DDS, SDS, HeRS, and the sub- M_{Ch} scenario for three different CE realizations. Within the framework of our adopted models, we find that only two

SN Ia formation scenarios are capable of matching the observed SNe Ia rates: the DDS and the sub- M_{Ch} channels. The most favourable model in terms of matching observational rates is model A1 ($\alpha \times \lambda = 1$). For models A1 and G1.5 ($\gamma = 1.5$), the adopted sub- M_{Ch} scenario is dominant at nearly all epochs $\lesssim 5$ Gyr, however the sub- M_{Ch} channel rate is too low for our low-efficiency CE model (A.125). For Model A.125, no single progenitor, nor an admixture of all of the progenitors combined are able to account for the observed rates of SNe Ia.

4.1 Nature of the progenitors: initial masses

In Figure 1, Figure 2 and Figure 3 we show the ZAMS masses of the primary (initially more massive star at birth) and secondary stellar masses for the DDS, SDS, HeRS and sub- M_{Ch} channels for Models A1, A.125 and G1.5, respectively. Note that the scales on the y -axes differ for all panels; the consequences of the CE model on the rates will be discussed in section 4.3.

Model A1 (standard model). The DDS progenitors, shown in Figure 1 panel *a*, originate from a wide range of ZAMS masses. It is clear from comparing Fig. 1*a* with the other panels that the DDS progenitors originate from binaries in which the initial mass ratio is on the order of unity for a large number of systems. For initial ZAMS mass ratios $q = M_{\text{primary}}/M_{\text{secondary}}$ close to unity, mass transfer is often stable and thus a CE event is avoided when the primary first fills its Roche-Lobe. The mass loss experienced by the primary star enables the formation of a CO WD (and not an ONeMg WD) even for initial ZAMS masses $> 8 M_{\odot}$. The mass gain⁸ experienced by the secondary star during the first RLOF serves to decrease the mass ratio q , so that when the secondary evolves off of the MS and fills its Roche-Lobe mass transfer (to the less massive primary WD) is unstable and a CE event ensues. In our calculations, the majority ($\sim 90\%$) of DDS progenitors undergo only one CE event. However, for a smaller number of DDS progenitors ($\sim 10\%$), initial mass ratios $q \gtrsim 1.7$, causing the first mass transfer phase to be unstable, and so the first CE phase is encountered when the primary first fills its Roche-Lobe, and a second one occurs after the secondary fills its Roche-Lobe.

For the SDS (Fig. 1 panel *b*), the primary and secondary mass components originate from two clearly distinctive populations: those with ZAMS masses above and below ~ 3 – $4 M_{\odot}$, respectively. The ZAMS secondary mass range lies between $0.5 < M_{\text{don,ZAMS}} < 2.8 M_{\odot}$. In most cases, the binary undergoes a CE phase when the primary is an asymptotic giant branch (AGB) star, though for the systems with the most massive (and thus more rapidly-evolving) primary progenitors with $8.5 < M_{\text{pri,ZAMS}} < 9.5 M_{\odot}$, the CE phase begins when the primary is a red giant (a similar evolutionary channel was addressed in Hachisu et al. 1999).

⁸ The amount of mass gained by the companion is uncertain. For all of our models, when a MS companion accretes from a mass-losing primary star during RLOF, we assume that 50% of the mass (Meurs & van den Heuvel 1989, see also study by Mennekens et al. 2010) is gained and the rest of the matter is lost from the binary carrying away angular momentum with the specific angular momentum of the accretor.

⁷ We note here that the γ CE equation in Belczynski et al. (2008, equation 55) is missing an exponent, though the CE evolution is properly carried out in the *StarTrack* code with the correct equation.

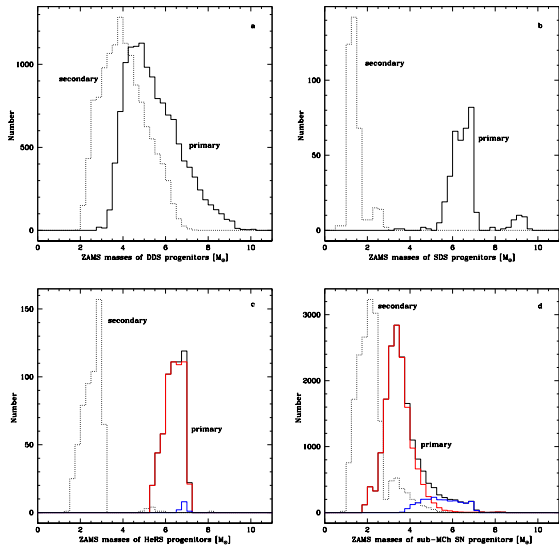


Figure 1. Progenitor (ZAMS) masses for primary (usually initially more massive star), and secondary stars for the SN Ia progenitors for Model A1. Panels from top-left: *a* (DDS); *b* (SDS); *c* (HeRS) and *d* (sub-Chandrasekhar). Red and blue lines indicate the ZAMS primary masses which correspond to SNe Ia involving WD and helium star donors, respectively. Note the different scales on the *y*-axes.

The red giant stars have helium-rich cores, and had they been single stars (or in very wide binaries) and able to maintain their envelopes during helium-shell burning, the red giant would continue adding mass to the helium core as it evolves on the red giant branch (RGB). However when mass loss occurs during the CE phase, evolution is truncated on the RGB, and instead the star is stripped of its hydrogen-rich envelope and a naked helium-burning star ($M_{\text{core}} = M_{\text{WD}} > 0.35 M_{\odot}$) is left in a binary with the companion (still on the MS). Since the naked helium star is still massive enough to burn helium, burning continues. These SDS SN Ia progenitors for which the CE phase occurs when the primary is on the RGB also undergo an additional phase of RLOF between the (evolved) naked helium star and the MS companion. Once the primary star has processed the helium into burning products (e.g., carbon and oxygen), it becomes a degenerate CO WD. Following the formation of the primary WD, the evolution for the SDS is basically the same for all binaries: the secondary fills its Roche-Lobe when it is on the Hertzsprung gap, RGB, or occasionally while it is on the MS, and the CO WD accretes hydrogen (the accretion efficiency and rate depend on the system parameters, see section 2 of Paper I), until the WD reaches M_{Ch} , at which point we assume the system explodes as a SN Ia.

The HeRS progenitors also show two relatively-distinct populations of initial mass (see panel *c* of Fig. 1). All of these progenitors undergo two CE events, and consist of CO WD accretors with either helium-burning stars or helium or hybrid WDs. The most common progenitors involve binaries where the donor is a WD. Helium WD donor systems involve the least-massive ZAMS donor masses: $1.4 < M_{\text{don,ZAMS}} < 2.6 M_{\odot}$. Progenitors that consist of a hybrid WD donor at the time of SN Ia originate from binaries where the donor

ZAMS mass was $2.4 < M_{\text{don,ZAMS}} < 3.1 M_{\odot}$. These systems start their last RLOF phase when the donor is a compact naked helium star (from a red giant which was stripped of its envelope), and lose enough matter such that the helium star mass drops below $0.35 M_{\odot}$, thus becoming a (degenerate) hybrid WD. The systems that have helium star donors at the time of SN Ia originate from the most massive secondaries on the ZAMS ($5.0 < M_{\text{don,ZAMS}} < 5.8 M_{\odot}$). The upper limit in primary ZAMS masses ($\sim 7 M_{\odot}$) corresponds to the mass above which the primary WD would become an ONeMg WD for this evolutionary channel.

The initial ZAMS mass distribution for the sub- M_{Ch} scenario SNe Ia are shown in Fig. 1, panel *d*. There is overlap between the sub- M_{Ch} channel and the HeRS channel; all of these progenitors contain helium-rich donors. However, contrary to panel *c*, the two main HeRS populations – WD donor and helium star donor – are more blended and no wide gap exists between the secondary and primary distributions. This is partially due to the fact that for the sub- M_{Ch} channel the mass of the WD at the start of the last RLOF phase can be as low as $\sim 0.6 M_{\odot}$, and thus the primary ZAMS progenitors can extend down to $1.9 M_{\odot}$. Nearly all binaries which have initial ZAMS secondary masses $> 3.0 M_{\odot}$, for which there are very few in panel *c*, produce sub- M_{Ch} SN Ia when the donor is a naked helium star (initial accretion rates are in the lowest accretion regime, Kato & Hachisu 2004). The narrow gap in secondary mass $\sim 3 M_{\odot}$ corresponds to the least massive secondary star mass which produces progenitors from the helium star branch, which is $\sim 2.7 M_{\odot}$. Below this mass, all systems become double WDs (mostly CO–He double WDs). Above this mass the majority have helium star donors, though a small number of hybrid WD donors exist here too. Similar to the HeRS channel, sub- M_{Ch} progenitors undergo two CE events before a stable phase of RLOF is encountered. However for many of the binaries involving hybrid WD donors, the ZAMS mass ratio is initially ~ 1 with both ZAMS masses $\sim 2.0\text{--}2.4 M_{\odot}$. Thus, the primary loses sufficient mass to the secondary star during RLOF such that the secondary star becomes the CO WD. These systems typically only undergo one CE event throughout their evolution.

Model A.125. Initial ZAMS mass distributions for the DDS (Fig. 2*a*) show even more overlap than for Model A1. For this model, all double-WD systems only undergo one CE event; those which undergo two CEs do not produce DDS progenitors since they merge out of the population too early and never make double WDs. The main evolutionary channel for the DDS in this model is different from that of the standard model, in that often the donor is at a more evolved stage at the start of the RLOF phase (usually an early AGB star rather than a sub-giant). Even though the initial mass distributions are very similar to those of Model A1, the systems which evolve into SN Ia progenitors in Model A.125 originate from binaries whose semi-lata recta [$a_0 \times (1 - (e_0)^2)$, where a_0 is the initial separation and e_0 is the initial eccentricity] are rather large in comparison to those of progenitors in the standard model (on the order of $150\text{--}250 R_{\odot}$ rather than $30\text{--}100 R_{\odot}$). Thus, the secondary stars are able to evolve and expand to giants or AGB stars before any mass exchange occurs, whereas the binaries with initially smaller semi-lata recta in Model A.125 will not survive the CE phase.

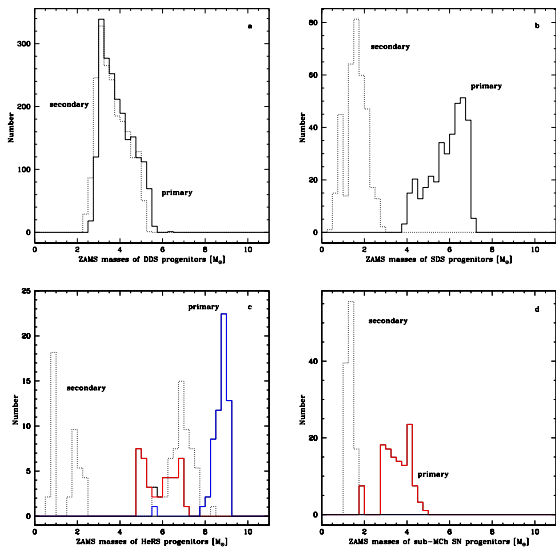


Figure 2. Same as Figure 1 for our A.125 model. Panels from top-left: *a* (DDS); *b* (SDS); *c* (HeRS) and *d* (sub-Chandrasekhar).

For the SDS (Fig. 2*b*), there are no progenitors which originate from systems with primary ZAMS masses $>8 M_{\odot}$, since these binaries will merge during the CE. However, for this model relatively more systems (for a given ZAMS range) will produce SNe Ia, since the lower CE efficiency more effectively brings the stars together following the CE phase. Thus, there is less time needed before stable RLOF can begin.

The HeRS scenario ZAMS mass range is quite different (Fig. 2*c*) than for the standard model. This CE model enables a variety of evolutionary channels to lead to the formation of SNe Ia which are not realised in the standard model. Systems with initial secondary masses $<1 M_{\odot}$ are formed through an ‘evolved low-mass MS donor’ channel, in which a low-mass MS star loses a significant amount of its hydrogen-rich envelope during RLOF while it continues to burn hydrogen in the core. Once the envelope is removed by mass transfer, what remains is an inert helium core.

The sub- M_{Ch} channel ZAMS distribution (Fig. 2*d*) looks quite different when compared to the standard model. There are no SNe Ia formed with initial secondary masses $\gtrsim 2 M_{\odot}$, and the primary ZAMS mass range is also narrower than for Model A1. This lack of higher mass secondaries results in an absence of SNe Ia from the channel with helium star donors. Stars which would have formed helium star channel sub- M_{Ch} SNe Ia in Model A1 can end up undergoing unstable mass transfer too early in the binary evolution; when the secondary is still on the MS. Due to the low CE efficiency, post-CE separations are small and consequently, the surviving sub- M_{Ch} progenitors are only able to form from binaries with ZAMS semi-latera recta which are rather large ($\gtrsim 1200 R_{\odot}$; though hybrid WD progenitors evolve through a different channel and their initial semi-latera recta are $\sim 70 R_{\odot}$).

Model G1.5. The DDS distribution (Fig. 3*a*) looks quite different when compared to the previous two models.

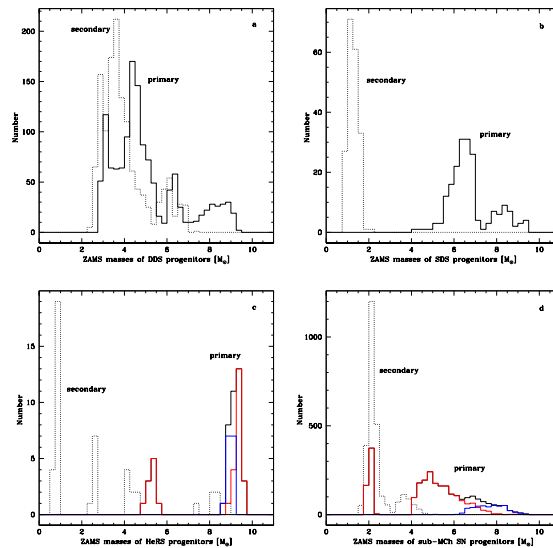


Figure 3. Same as Figure 1 for our G1.5 model. Panels from top-left: *a* (DDS); *b* (SDS); *c* (HeRS) and *d* (sub-Chandrasekhar).

In this CE parametrization, the post-CE separation of all binaries is fairly large and thus often the stars never make SN Ia progenitors. Having said that, the fact that post-CE separations are large enables systems that would have merged after two CE events in Model A1 to survive and produce DDS SNe Ia in this model. Thus, a wide variety of evolutionary pathways exist for Ia progenitors in this model. Additionally, these progenitors originate from a rather wide range of semi-latera recta (~ 50 to a few hundred R_{\odot}).

The SDS ZAMS distributions (Fig. 3*b*) are quite similar to those of Model A1, and thus the evolutionary channels are roughly the same (the main difference is apparent in the DTD; section 4.2).

The HeRS ZAMS mass distribution (Fig. 3*c*) is roughly similar to that of Model A.125, although there is hardly any overlap between primary and secondary ZAMS masses, and thus (almost) every HeRS progenitor begins its evolutionary sequence with a CE phase. This model produces some SNe Ia from low-mass donors ($M_{\text{don,ZAMS}} < 1 M_{\odot}$) through an evolutionary sequence which is very similar to those found in Model A.125 but not found in Model A1 (discussed above). However in this case the progenitor undergoes two CE events rather than one before stable RLOF begins.

The ZAMS mass distributions of the sub- M_{Ch} progenitors (Fig. 3*d*) have a shape somewhat similar to that of Model A1, though shifted to higher masses and with a narrower range of secondary masses. The formation channels are similar to those described for the standard model, though there is a clear lack of systems with primary ZAMS masses $\sim 2-4 M_{\odot}$. These binaries, which would have made sub- M_{Ch} in the standard model, usually end up only undergoing one CE event and form detached CO WDs.

4.1.1 typical evolution

In Figure 4 we present the mass and mass transfer evolution as a function of time for a typical sub- M_{Ch} SN Ia from our population synthesis Model A1, with final WD masses 1.07 and $0.02 M_{\odot}$, respectively. In the top panel we show the mass evolution of the stars. The ZAMS masses of the stellar components are 3.55 and $2.13 M_{\odot}$. The first CE event occurs at 298 Myr when the primary is a thermally-pulsating AGB star, which leaves behind a CO WD, and the secondary is on the MS. A second CE occurs at 1000 Myr when the secondary is a red giant, leaving behind a newly-formed helium WD (degenerate core of the red giant). Within 13 Myr, the two WDs are brought into contact by gravitational wave radiation (initial mass transfer rate $\sim 2 \times 10^{-5} M_{\odot} \text{ yr}^{-1}$), and an AM CVn system is born. As the orbital period increases during mass transfer, the mass accretion rate rapidly decreases (Fig. 4, bottom panel). The sub- M_{Ch} accretion regime for this system is reached when the mass transfer rate is $\sim 10^{-7} M_{\odot} \text{ yr}^{-1}$. Even though in this regime helium accretion is fully efficient, due to the decreasing mass transfer rate the binary spends another ~ 240 Myr in RLOF before a $0.1 M_{\odot}$ layer of helium is accumulated on the WD surface and a sub- M_{Ch} SN Ia ensues.

If a low CE efficiency is assumed for the same binary (Model A.125), a SN is never produced. Instead, the system merges shortly after the first CE, when the (post-ABG) primary is a CO WD and the secondary is on the MS. A merger occurs since upon emerging from the CE, the spin angular momentum of the binary is more than $\frac{1}{3}$ of the binary orbital angular momentum, leading to a (Darwin) dynamical instability. Such mergers are interesting for stellar and binary evolution, though they are unlikely to make normal SNe Ia.

If the γ prescription is assumed (Model G1.5) a SN is never produced either, since after the CE event the size of the orbit only decreases by $\sim 20\%$ (not 95% as is the case in Model A1). At this large post-CE separation ($800 R_{\odot}$; an orbital period of 4.25 years) the stars are not close enough for interactive evolution when the secondary evolves off of the MS and fills its Roche-Lobe at ~ 1270 Myr. Thus the system becomes a detached COWD-COWD binary, with component masses 0.80 and $0.64 M_{\odot}$. While the total mass is high enough to possibly result in a DDS SN Ia if the system merges, the separation is too wide and the stars will remain a detached double WD for well over a Hubble time.

4.2 Delay times

In Figure 5 we show the delay time distribution of the four aforementioned progenitor channels for Models A1, A.125 and Model G1.5. We note that the bumpiness in the smoothed plot is due to Monte Carlo noise. For our DTD normalisation of all models, we have assumed a binary fraction across the entire initial stellar mass function of 50% ($\frac{2}{3}$ of stars are in binaries), and we show the DTD normalised to stellar mass (SNuM and $\text{SNe yr}^{-1} M_{\odot}^{-1}$). The mass represents the mass in formed stars, which includes mass which has potentially been expelled from stars in SNe or thermal pulses for example. In section 4.3, we give the delay times in tabular form.

Along with our theoretical DTDs, we show the observed

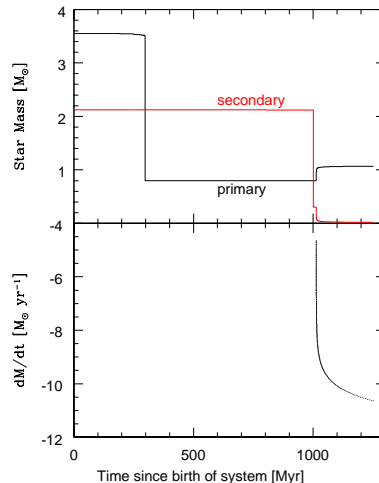


Figure 4. Characteristic evolution of a sub- M_{Ch} SN Ia from our *StarTrack* models. The two steep drops in mass at $t \sim 300$ Myr and ~ 1000 Myr (top panel) coincide with the two CE events, each one leading to a substantial decrease in orbital period by \gtrsim an order of magnitude. RLOF starts ~ 1013 Myr, and over the course of RLOF the orbit widens and the mass transfer rate decreases (bottom panel). Initial mass transfer rates are very high ($\sim 10^{-5} - 10^{-6} M_{\odot} \text{ yr}^{-1}$), typical of double white dwarf systems which have just started RLOF, since the separation is small once contact is established (a few minutes orbital period). Notice that the primary WD accretes (and burns) more than $0.1 M_{\odot}$ of helium before the final $0.1 M_{\odot}$ helium shell is accumulated.

(cosmic) DTD from the literature (Maoz et al. 2010a). We wish only to compare the relative DTD shapes and not the absolute rates, since the normalisation of our *StarTrack* DTD differs substantially from the normalisation techniques used in recovering the various observational DTDs. The difference between the (higher) rates of observed SNe Ia and the rates from population synthesis is visible, and the apparent discrepancy is not yet fully resolved. It has been suggested that binary population synthesis codes tend to under-predict the SN Ia rates compared to the rates inferred from recent observations, though one must keep in mind that many uncertainties are associated with the DTD recovery methods, i.e., extinction, star formation history, and the use of spectral population synthesis codes which neglect the existence of binaries (see De Donder & Vanbeveren (2004), also Eldridge & Stanway (2009) have found that inclusion of massive binaries in spectral synthesis codes plays an important role in recovering accurate host galaxy properties).

Model A1. As was found in Paper I Model 1, the DDS distribution for Model A1 (top panel of Figure 5) follows a power-law distribution with $\sim t^{-1}$ (see also Figure 6), while the SDS distribution is somewhat flat with no events with delay times less than 460 Myr. The reason why the SDS does not harbour very prompt events is directly linked to the donor star’s initial ZAMS mass. When the secondary ZAMS mass is $> 2.8 M_{\odot}$, the binary will enter a CE phase when the secondary fills its Roche-Lobe, rather than a stable

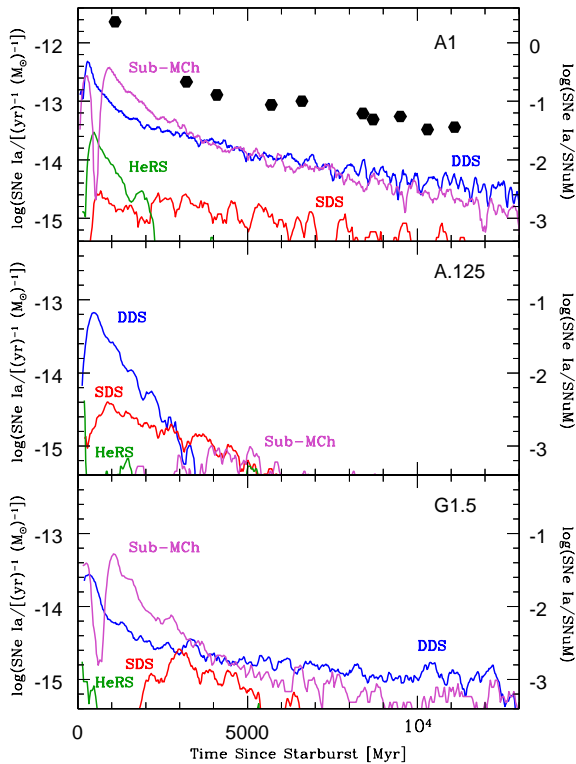


Figure 5. Lines represent the DTD for SNe Ia. Top panel: Model A1. Middle panel: Model A.125. Bottom panel: Model G1.5. The number of SNe Ia per year per unit stellar mass born in stars (at starburst $t = 0$, 50% binarity) is shown for the DDS (blue), SDS (red), HeRS (green), and sub- M_{Ch} (magenta) channels. The sub- M_{Ch} SN Ia DTD clearly shows two distinct populations for Models A1 and G1.5: the helium star channel (spike at delay times $\lesssim 500$ Myr) and the WD channel (from ~ 800 Myr to a Hubble time). The helium star channel however is absent in Model A.125. In the top panel we additionally show the DTD [SNU[M]] compiled by Maoz et al. (2010a, table 1), which is fit relatively well by a power-law $\sim t^{-1.2}$. The data points showing the observed DTD are computed using a different normalisation technique (see text), and thus we show the points for comparison of the DTD shapes and not the absolute numbers. We note that assuming a different binary fraction or IMF would change the level of our normalisation.

RLOF phase. In such a case, the binary will not become an SDS SN Ia, though may under the right circumstances evolve to SN Ia from the HeRS channel (compare secondary mass distributions of Panels *b* and *c* of Fig. 1). The SDS events at long delay times originate from progenitors with very low-mass MS donors, which take many Gyr to evolve to contact under the influence of magnetic braking. The HeRS DTD consists mostly of systems with relatively short (~ 100 Myr–2 Gyr) delay times, with very few events at longer delay times. We refer the reader to Paper I for a description of these DTDs.

The sub- M_{Ch} systems can easily by eye be grouped into two classes: those prompt SNe which occur with delay times $\lesssim 500$ Myr, and those with delay times above ~ 800 Myr, with very little overlap. Not surprisingly, these two classes of SNe Ia stem from two very different formation scenarios.

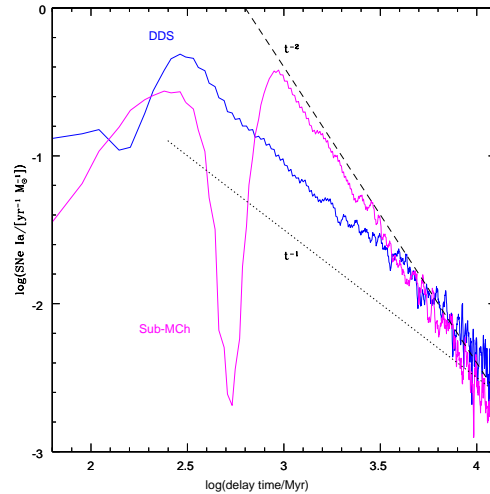


Figure 6. Delay time distribution for the DDS (blue) and sub- M_{Ch} (magenta) channels for model A1 (standard). We show two power-laws alongside the DTDs: the DDS is relatively well-fit by a power-law t^{-1} , whereas the sub- M_{Ch} model closely follows a power-law with t^{-2} beyond 1 Gyr, where all progenitors have helium-rich WD donors.

Those with short delay times consist of progenitors which involve a helium-burning star donor, whereas the rest mainly consists of helium WD donors (systems with hybrid WD donors span ~ 0.3 –3 Gyr delay times). We find that progenitors with helium star, helium WD and hybrid WD donors comprise 12.5%, 78.3% and 9.2% of SNe Ia, respectively.

The prompt component accounts for 13% of all sub- M_{Ch} SNe Ia that explode within 13 Gyr of star formation. Nearly all of these systems (96%) have helium star donors, with the rest having hybrid WD donors. The delay time is governed by the MS lifetime of the donor star. The companions with ZAMS masses $\gtrsim 3 M_{\odot}$ evolve off of the MS within $\lesssim 400$ Myr. After the first CE, which leaves behind a CO primary WD and a MS secondary star, the secondary (e.g., on the Hertzsprung gap) will fill its Roche-Lobe and mass transfer is once again unstable leading to a second CE phase. The CE leaves the CO WD and newly-formed naked helium star on a close orbit (~ 35 –40 min). Within a few Myr, the orbit decreases to ~ 25 min, and the helium star fills its Roche-Lobe. However, initial mass transfer rates for the helium star channel are low enough to enable accumulation of the helium shell to commence immediately: typically such systems have initial mass transfer rates $\sim 2 \times 10^{-8} M_{\odot} \text{ yr}^{-1}$ (for a discussion on the evolution of low mass helium stars in accreting binaries see Yungelson 2008).

The delayed component (delay times > 500 Myr) comprise the other $\sim 87\%$ of the sub- M_{Ch} progenitors. Binaries with helium WD donors make up 90% of the delayed component, while 10% have hybrid donors. These binaries also evolve through two CE phases, as is expected for the evolution of AM CVn binaries. Similar to the DDS, the time-scale governing the DTD for the helium WD channel is largely set by the gravitational radiation time-scale. However unlike the DDS, these WDs do not merge upon contact, but enter a stable phase of RLOF. Like the DDS DTD, the sub- M_{Ch} DTD

follows a power-law above 1 Gyr, however with a steeper functional form of t^{-2} (Figure 6, see also section 5.2).

Model A.125. In the middle panel of Figure 5, we show the DTD for Model A.125. Contrary to the standard model, the DDS DTD is lacking progenitors at longer delay times since on average the time a progenitor spends as a detached double WD is decreased in this model (smaller orbital separation following the CE phase). For this model the SDS progenitors can have shorter delay times compared to the standard model due to the fact that the post-CE separations are overall smaller. Thus, a low CE efficiency model is more favourable for the production of SDS SNe Ia. The HeRS channel has some very prompt events (helium star channel), although the low CE efficiency serves to result in a merger during CE more frequently than in Model A1. The events at delay times ~ 1 –2 Gyr belong to progenitors with helium WDs, while events at long delay times ($>$ a few Gyr) also involve helium WDs but belong to the evolved low-mass MS donor channel discussed previously. The DTD of the sub- M_{Ch} progenitors looks drastically different from that of the standard model, and lacks a prompt component. This model is the only of the three which does not display a prominent division of the sub- M_{Ch} progenitor channels; in fact there are no sub- M_{Ch} SNe Ia originating from the helium star channel. As discussed in section 4.1, those progenitors will encounter unstable RLOF too early in their evolution. With the adopted CE prescription, it is very difficult (or impossible) to produce helium star donor channel sub- M_{Ch} SNe Ia within our model framework, and thus there are no prompt events (the first SN Ia from the sub- M_{Ch} channel occurs at ~ 1.7 Gyr).

Model G1.5. In Figure 5, bottom panel, we show the DTD for Model G1.5. Gravitational radiation plays a less significant role for the DDS since following the CE phase the binary orbit is still rather wide. Similar to the other two models, the DDS contributes the majority of its events at very early times followed by a decline. The SDS channel displays no prompt events, because the first CE event does not lead to a dramatic decrease in orbital separation. In general, the SNe Ia with short SDS delay times from Model A1 will evolve into detached double CO WDs in Model G1.5, since the binary orbit is not small enough for mass transfer to begin once the secondary evolves off of the MS and fills its Roche-Lobe. The HeRS channel leads to SNe Ia with very short delay times, though there are events at long delay times but their frequency is for the most part too low to be seen on Fig. 5. The sub- M_{Ch} DTD has the same general shape as Model A1: the prompt and the delayed components. We note however that SNe Ia with delay times less than 1 Gyr follow a different evolutionary sequence compared to the corresponding events of Model A1. In Model A1, the first mass exchange interaction occurs when the primary is an AGB star, whereas for Model G1.5 the first mass exchange event (CE or stable RLOF) occurs when the primary is less evolved; a sub-giant or giant. This occurs since the semi-lata recta (and thus in general, the separations) of the G1.5 sub- M_{Ch} progenitors are smaller when mass transfer begins, as well as the fact that the primaries for this model are somewhat more massive than compared to the standard model and thus they evolve more quickly (compare ZAMS primary distributions of Figs. 1d and 3d).

Table 1. Rates of SNe Ia (SNUM, 50% binarity) for the four progenitor formation scenarios considered in this work, following a starburst at $t = 0$. Models A1 (left), A.125 (middle) and G1.5 (right).

	A1	A.125	G1.5
DDS			
0.1 Gyr	2.0×10^{-1}	$< 10^{-4}$	2.0×10^{-2}
0.5 Gyr	1.6×10^{-1}	6.5×10^{-2}	2.2×10^{-2}
1 Gyr	8.0×10^{-2}	2.5×10^{-2}	5.3×10^{-3}
3 Gyr	2.5×10^{-2}	$\lesssim 10^{-4}$	$\sim 2 \times 10^{-3}$
5 Gyr	1.2×10^{-2}	0	$\sim 2 \times 10^{-3}$
10 Gyr	$\sim 5 \times 10^{-3}$	0	$\lesssim 10^{-3}$
SDS			
0.1 Gyr	0	10^{-3}	0
0.5 Gyr	$\sim 10^{-3}$	3.5×10^{-3}	0
1 Gyr	1.5×10^{-3}	5×10^{-3}	$\lesssim 10^{-3}$
3 Gyr	2.0×10^{-3}	$\lesssim 10^{-4}$	$\sim 2 \times 10^{-3}$
5 Gyr	$\sim 1 \times 10^{-3}$	$< 10^{-4}$	$\sim 10^{-4}$
10 Gyr	$\lesssim 10^{-3}$	~ 0	$\lesssim 10^{-4}$
HeRS			
0.1 Gyr	$\sim 3 \times 10^{-3}$	4×10^{-3}	$\lesssim 10^{-3}$
0.5 Gyr	2.2×10^{-2}	0	$< 10^{-3}$
1 Gyr	8.0×10^{-3}	$< 10^{-3}$	$< 10^{-4}$
3 Gyr	$< 10^{-3}$	$\lesssim 0$	$< 10^{-4}$
5 Gyr	$\lesssim 10^{-4}$	$< 10^{-4}$	$< 10^{-4}$
10 Gyr	~ 0	~ 0	$< 10^{-4}$
sub-M_{Ch}			
0.1 Gyr	$\sim 1 \times 10^{-1}$	0	$\lesssim 10^{-4}$
0.5 Gyr	$\sim 10^{-3}$	0	$\sim 10^{-3}$
1 Gyr	3.3×10^{-1}	$< 10^{-4}$	$\sim 7 \times 10^{-2}$
3 Gyr	4.0×10^{-2}	$< 10^{-4}$	$\sim 4 \times 10^{-3}$
5 Gyr	1.4×10^{-2}	$< 10^{-3}$	$\sim 2 \times 10^{-3}$
10 Gyr	$\sim 4 \times 10^{-3}$	~ 0	$\lesssim 10^{-4}$

4.3 Rates

In Table 1, we show the DTDs in tabular form (rates as a function of epoch) for our models. We estimate the Galactic SN Ia rate by convolving the DTD (in units of SNe/time) with a constant star formation history from 0–10 Gyr with a total mass born in stars of $6 \times 10^{10} M_{\odot}$; see section 4 of Paper I. In this paper, we do not quantify the Galactic rate estimates explicitly since imposing a particular star formation history serves to add sources of uncertainty to our DTD calculation, however we give some numbers as a guide. In principle, all of the important information is already presented in the DTD plots and Table 1: it is possible to convolve the specific DTD with any star formation history of choice in order to achieve a particular SN Ia rate for a given stellar population.

Model A1: This model produces the highest number of SNe Ia out of our 3 models. Table 1 (left) is very similar to table 1 (Elliptical column) in Paper I, though here for all tables we additionally include the rates of sub- M_{Ch} SNe Ia, as well as two additional epochs: 0.1 and 1 Gyr after star formation. Slight variations between the numbers in this study and table 1 of Paper I are due to a slight increase in volume of data, and thus a reduction in noise from low-number statistics. We find that the rate of our adopted sub- M_{Ch} SN Ia model exceeds all other progenitor channels between

~ 0.7 and 5 Gyr, and these systems are enough to account for the observed SN Ia rate, with a calculated Galactic rate of $\sim 2.6 \times 10^{-3}$ SN Ia yr $^{-1}$ (including all systems with a total WD mass $\gtrsim 0.9 M_{\odot}$). For comparison, the DDS rate is $\sim 2 \times 10^{-3}$ SN Ia yr $^{-1}$. Both of these values are within the estimate from Cappellaro et al. (1999) of $4 \pm 2 \times 10^{-3}$ SN Ia yr $^{-1}$. As was determined in Paper I, the Model A1 DDS rates are able to (just) account for the observed Galactic rate of SNe Ia, whereas both the SDS and HeRS channels fall short by over an order of magnitude.

Model A.125: This model produces the least SNe Ia progenitors out of our three models. The DDS is significantly decreased in number (Table 1, middle), but is still the dominant channel at most times under a few Gyr. The SDS rate exceeds the DDS rate above 3 Gyr, though the overall rates are still too low for any progenitor in this model to account the observed SN Ia rates. The rates of the HeRS SNe Ia are too low; many binaries do not survive both CE events to become progenitors. Similarly, as discussed in section 4.1, the sub- M_{Ch} progenitors are not easily formed in this Model.

Model G1.5: The overall rates for this model (Table 1, right) are lower than found in the standard model, though not as low as found for Model A.125. In the DDS, since the binaries take a longer time to reach contact (e.g., it can easily be more than a Hubble time), the overall SN Ia rates are rather low compared to Model A1 with an estimated Galactic rate of $\sim 2 \times 10^{-4}$ yr $^{-1}$, which is about a factor of 10 too low. The SDS channel produces very few events before 2 Gyr, and matches those of the DDS at ~ 3 Gyr, while the HeRS channel produces events with delay times < 1 Gyr and few events at later times. Even though the sub- M_{Ch} DTD exhibits the same general shape as found in the standard model, the rates are overall too low being roughly comparable to those of the DDS of this model (Galactic rate estimate $\sim 3 \times 10^{-4}$ yr $^{-1}$).

4.4 CO core masses

In the sub- M_{Ch} scenario, the brightness is expected to be largely determined by the mass of the underlying CO WD. In Figure 7, we show the mass of the CO WD ‘core’ (total WD mass minus the helium shell mass) at time of SN Ia. As mentioned previously, a detonation of a $\sim 0.7 M_{\odot}$ core WD would likely not look like a normal SN Ia. Since we currently lack a theoretical lower mass limit for which exploding CO core masses could potentially exhibit features which are characteristic of SNe Ia, for completeness we show the CO core mass at explosion for the entire mass spectrum for exploding sub- M_{Ch} cores. We draw a vertical line at $M_{\text{core}} = 0.8 M_{\odot}$, above which the systems are considered to be sub- M_{Ch} SNe Ia in our models.

The core mass distributions look very different for all three models. In the top panel of Figure 7, we show the core mass distribution for Model A1. The progenitors of binaries with low core masses ($< 0.7 M_{\odot}$) go through a different evolutionary channel than those with higher core masses since they start out with smaller semi-lata recta and only evolve through one CE event. The cores associated with the helium star channel span both low and high masses, though for our adopted sub- M_{Ch} scenario they have slightly higher core masses on average compared to the WD channels. The hybrid WD channel shows a similarly flat distribution, which

is not unexpected since many of these systems undergo an evolutionary sequence which is like that of a typical progenitor from the helium star channel. For the helium WD channel which comprises the majority, the masses decrease fairly steadily in number with increasing mass, since there are simply a larger number of less-massive CO WD cores to start with. There is a clear lack of CO core masses below $\sim 0.7 M_{\odot}$. Typically these CO core progenitors will accrete (and burn) at least $0.1 M_{\odot}$ (often $\sim 0.2 M_{\odot}$) of helium at a high accretion rate before the phase of helium accumulation begins for the $0.1 M_{\odot}$ shell, and thus we find no CO cores from this channel with very low masses. However, there are a number of exploding cores with masses $\sim 0.7 - 0.8 M_{\odot}$. One has to also consider the possibility that a low-mass ($< 0.8 M_{\odot}$) CO core + helium shell may not reach sufficient conditions for a detonation to take place, which might explain why we would not see a large number of these events.

For Model A.125 (Figure 7, middle panel), the separation between the helium star and double WD channels is quite distinct. The lowest mass CO cores belong to progenitors with helium star donors, and in our adopted sub- M_{Ch} model all of these binaries have CO core masses which are too low to qualify as SNe Ia. The ZAMS masses of these CO cores are small, $\sim 1.8 - 2.1 M_{\odot}$,⁹ and these stars are unable to build a massive CO core before the first CE is encountered. Additionally, binaries which start their final RLOF phase when the secondary is a helium star have lower initial accretion rates ($\sim 10^{-8} M_{\odot}$ yr $^{-1}$), which allows the CO core to immediately accumulate (not burn) a shell of helium and produce a SN Ia without the CO WD having to grow in mass by an extra $\sim 0.1 - 0.2 M_{\odot}$.

The distribution of CO core mass for the helium WD channel of Model G1.5 (Figure 7, bottom panel) is very similar to that of the standard model. However the different evolutionary sequences allowed in this model enable the formation of more progenitors involving hybrid WD donors. The mass distributions for the helium star and hybrid WD channels peak between 0.85 and $0.9 M_{\odot}$ (total WD mass $0.95 - 1 M_{\odot}$), which is a noteworthy feature, especially if these systems are shown to contribute to the population of SNe Ia of ‘normal’ brightness (Sim et al. 2010).

5 DISCUSSION

Recent hydrodynamic explosion simulations of sub- M_{Ch} CO WDs (Fink et al. 2010) coupled with detailed nucleosynthesis and radiative transfer modelling (Kromer & Sim 2009) have revealed that sub- M_{Ch} mass SN Ia models exhibit features which are characteristically similar to those observed in SNe Ia (Sim et al. 2010; Kromer et al. 2010). Motivated by these new findings, as well as population synthesis rate estimates, we have investigated sub- M_{Ch} SN Ia formation channels and have calculated and presented the delay time

⁹ In Fig. 2d, one can see that there are sub- M_{Ch} progenitors which have primary ZAMS masses $\sim 2 M_{\odot}$, however these binaries follow a different evolution due to their initial separations and mass ratios, and thus the primary progenitors are able to evolve well into the late AGB phase and build up a relatively massive CO core before the first CE event occurs.

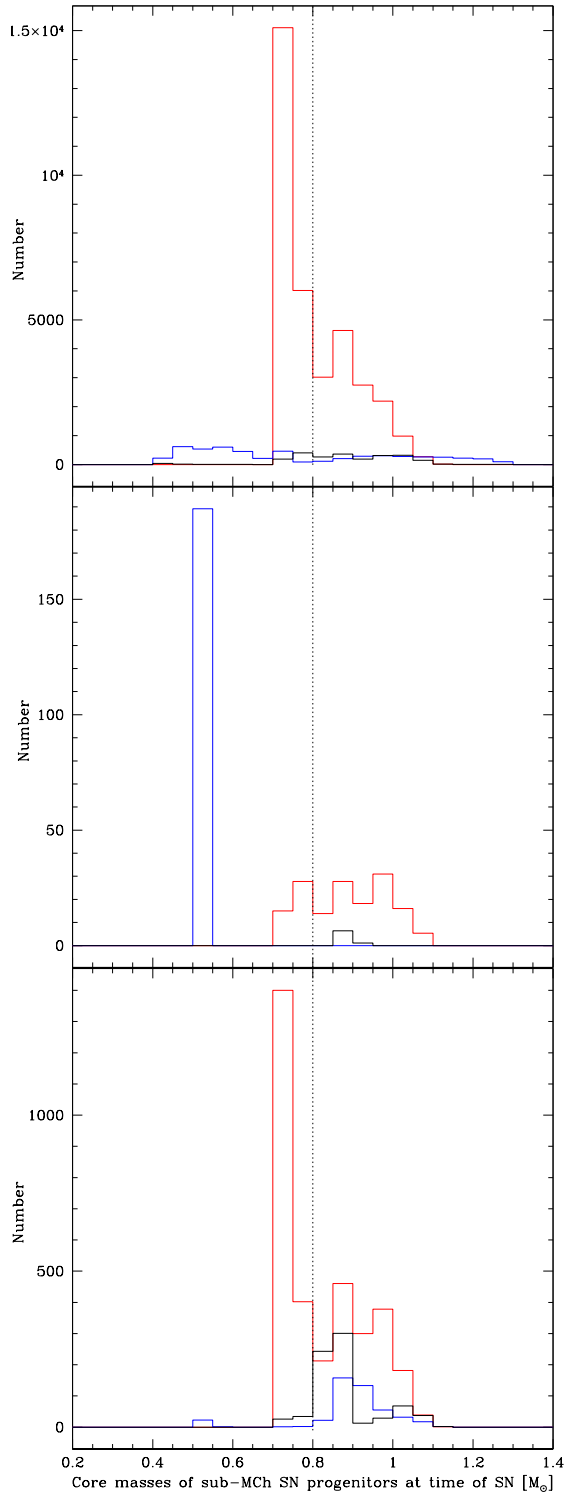


Figure 7. Distribution of StarTrack CO WD core masses which managed to accumulate a $0.1 M_{\odot}$ shell of helium. A double-detonation was assumed to follow in all cases. A vertical line is drawn at $M_{\text{COcore}} = 0.8 M_{\odot}$, above which all systems are assumed to lead to sub- M_{Ch} SN Ia in our three models ($M_{\text{COcore}} + M_{\text{He shell}} = \text{total WD mass}$). Top panel: Model A1. Middle panel: Model A.125. Bottom panel: Model G1.5. The helium star channel is outlined in blue, the He-WD channel is outlined in red and the hybrid WD channel is outlined in black. Note different scales on the y -axes.

distribution and rates of their progenitors for three different parametrizations of the common envelope phase.

We find that only the sub- M_{Ch} progenitor channel is able to simultaneously

- reproduce the observed rates for our standard model
- provide an elegant explanation for the variety among SN Ia light-curves (mass of exploding WD)
- naturally provide a system which is devoid of hydrogen
- produce a DTD with distinct prompt ($\lesssim 500$ Myr)¹⁰ and delayed ($\gtrsim 500$ Myr) components, originating from two channels with very different evolutionary time-scales

We think that this last point is one of the most interesting, considering the recent observational studies by different groups who have found evidence for such a DTD (Brandt et al. 2010; Maoz & Badenes 2010; Maoz et al. 2010b).

5.1 Double white dwarf mergers: implications

We note both the works of Guillochon et al. (2010), who investigated detonations in sub- M_{Ch} CO WDs undergoing rapid accretion during dynamically unstable mass transfer from a helium-rich WD companion, and van Kerkwijk et al. (2010), who also considered mergers of WDs with a total mass below M_{Ch} as possible progenitors of SNe Ia. In this study we do not investigate sub- M_{Ch} mergers in detail though we briefly comment on them here. We find that the number of sub- M_{Ch} WD mergers in our standard model (considering all mergers where at least one WD is CO-rich, the other being CO and/or helium-rich) is nearly twice that of DDS mergers. While it is generally believed that a WD merger with a total mass below the Chandrasekhar mass limit would not lead to a SN Ia explosion, these mergers should produce other interesting objects; R Coronae Borealis stars are one example (Webbink 1984; Clayton et al. 2007, see also Bogomazov & Tutukov (2009)) and these types of merger events may be visible in upcoming transient surveys. If we make a constraint similar to that of van Kerkwijk et al. (2010) counting both sub- M_{Ch} and super- M_{Ch} WD mergers between CO WDs with near-equal masses, we find that the number of mergers drops to $\sim 42\%$ of our standard model DDS rate, which is slightly too low to explain all SNe Ia.

In our models we have assumed the commonly-adopted initial binary orbital configurations for population synthesis studies: i.e., initial separation flat in the logarithm (more binaries born on closer orbits relative to large orbits), and thus the ZAMS distribution of all semi-lata recta are the same for all three CE models. However, we find that for the low-CE efficiency case (Model A.125), DDS SNe Ia progenitors are only formed from systems with initial (ZAMS) orbital configurations which have rather large semi-lata recta compared to those for our standard model. In Model A.125, systems which would have made DDS SNe Ia in Model A1 merge too early, and never make double WDs. It was already mentioned in Hurley et al. (2002) that the initial distribution of orbital separations in population synthesis studies

¹⁰ We note that $\sim 35\%$ of sub- M_{Ch} SNe Ia in our models explode within 1 Gyr of star formation.

should be distributed according to the (observed) distribution of semi-latera recta rather than semi-major axes or orbital periods alone. We note here that an initial distribution geared toward higher semi-latera recta than is canonically assumed would serve to augment the number of progenitors in models with low CE efficiency, making those DDS rates closer to those of observations.

While the predicted rates of the DDS for our models do not conflict with observations, these systems are theoretically expected to produce neutron stars via AIC. If this were the case, the AIC rate from the AIC-merger channel alone would be $\sim 10^{-3}$ per year for the Galaxy. We find the **StarTrack** AIC rate from the ‘RLOF-AIC’ channel is a factor of 10 to 100 less: no more than 10^{-4} per year for our standard model. This rate is in agreement with the upper limit estimate derived from solar system abundances of neutron-rich isotopes, which are expected to be produced in AICs (Fryer et al. 1999; Metzger et al. 2009). However, if *i*) population synthesis estimates for the number of merging CO+CO WDs with a mass above M_{Ch} are correct and *ii*) in most environments these mergers preferentially produce AICs and not SNe Ia, then this could potentially be in conflict with the predicted abundance of neutron-rich isotopes in the solar neighbourhood. However, modelling of AIC events, be it the ‘RLOF’ or ‘merger’ case, is still in its infancy, and many uncertainties remain (Dessart et al. 2006, 2007; Metzger et al. 2009, see also Darbha et al. 2010). If one can say for certain that AIC events formed from the merger of CO WDs produce very neutron-rich ejecta, then this provides a potentially strong constraint on the outcome of these mergers; namely that a non-negligible fraction of SNe Ia must be formed through the DDS channel. On the other hand, it is possible that population synthesis calculations over-predict the number of merging CO+CO WDs, which would also present an interesting problem for the binary evolution community, and may challenge the idea that the observed $\sim t^{-1}$ power-law DTD of SNe Ia originates from double WD mergers alone.

5.2 Further remarks on delay times

The t^{-1} power-law shape found in the delay time study of Totani et al. (2008) implies that the majority of progenitors in elliptical-like galaxies originate from binaries for which the DTD is most strongly governed by the time-scale associated with gravitational wave radiation, thus these progenitors are likely to be DDS mergers (see section 3 of Ruiter et al. 2009). Similar to the DDS, our study has shown that the sub- M_{Ch} model DTD (e.g., Model A1) also exhibits a power-law for delay times >1 Gyr. This is not surprising, since the helium WD sub- M_{Ch} progenitors also spend an appreciable time as detached double WDs evolving to contact solely under the influence of gravitational radiation. However, the DTD of the sub- M_{Ch} channel falls off more steeply than the t^{-1} power-law fit of Totani et al. (2008) and the $t^{-1.1} - t^{-1.3}$ power-law fits of Maoz et al. (2010a), matching quite well to t^{-2} (Figure 6). Thus, when comparing our results to observationally-derived DTDs, the DDS channel matches more closely than the sub- M_{Ch} channel. However, a very recent study of Subaru/XMM-Newton Deep Survey (SXDS) SNe Ia indicates that the DTD may be well-fit by a power-law of $t^{-1.5}$ (J. Okumura, private communication

2010). It is of course possible that both DDS and sub- M_{Ch} progenitors contribute substantially to the SN Ia population, potentially yielding a DTD of functional form somewhere in between t^{-1} and t^{-2} above 1 Gyr, which would still be in agreement with the majority of recent observations.

5.3 Sub-Chandrasekhar SNe Ia connection to AM CVn stars and .Ia events

Based on the observed local space density estimate of AM CVn binaries¹¹ performed by Roelofs et al. (2007), Bildsten et al. (2007) have calculated the occurrence rate of the final (explosive) helium flash from ‘point Ia’ (.Ia) systems in a typical E/S0 galaxy with a mass of $10^{11} M_{\odot}$ to be $(7 - 20) \times 10^{-5} \text{ yr}^{-1}$; i.e., 2–6% of the SN Ia rate in E/S0 galaxies. Since our sub- M_{Ch} progenitors could also potentially lead to .Ia-like (and not SN Ia) explosions, we think it is useful to independently estimate the occurrence rate for such explosions in our standard (A1) model for similar (E/S0 galaxy) conditions.

We find that for a binary fraction of 50%, one sub- M_{Ch} occurs for every 2158 M_{\odot} born in stars (for 100% binarity, the yield is 1 sub- M_{Ch} Ia per 1324 M_{\odot}). Thus for a total mass born in stars of $10^{11} M_{\odot}$, up to 4.6×10^7 sub- M_{Ch} Ia are expected to occur over a Hubble time. How many SNe Ia actually occur crucially depends upon the assumed star formation history of the galaxy. If the birth times for these binaries are spread out evenly over the age of the galaxy (10 Gyr), as would be assumed for a constant star formation history, we find an average SN Ia rate of $<4.6 \times 10^{-3} \text{ yr}^{-1}$. This estimate is only an upper limit as most systems which were born at late times will not have time to evolve into SNe Ia by 10 Gyr. For the case of E/S0 galaxies, we expect that the star formation history would not be constant, but would have been much higher in the past. Hence the corresponding birth rate should decrease as a function of time (see fig. 2 of Ruiter et al. 2009). In this case, more binaries have enough time to evolve into SNe Ia over 10 Gyr, however the SN Ia rate will ‘die out’ at long delay times due to lack of star formation activity. These two effects serve to compete against each other. It was already found in section 4.3 that the sub- M_{Ch} rate assuming a burst of star formation at $t = 0$ is $\sim 4 \times 10^{-3}$ at 10 Gyr. Thus we find that among old stellar populations our sub- M_{Ch} Ia explosions will be roughly 30 times more frequent than the estimated .Ia explosion rate of Bildsten et al. (2007).

We also note that in the study of Bildsten et al. (2007) it was found that the ignition mass of the helium shell in .Ias varies as a function of the underlying CO core mass and the rate of accretion. However for our first investigation of double-detonation sub- M_{Ch} SNe we have used a more simplified model in which the ignition mass is always the same ($0.1 M_{\odot}$). The consequences of this on the resulting

¹¹ We would like to make the reader aware of the fact that population synthesis studies over-predict the number of AM CVn binaries in general compared to the observational results of Roelofs et al. (2007) (e.g., Nelemans et al. 2001; Ruiter et al. 2010). There may be several factors which conspire to cause the apparent difference, though the various possibilities are not explored in this study.

SN rate are not expected to be too drastic, as the time-scale for the helium accretion is relatively short compared to the evolutionary lifetime of the progenitors. This is particularly true for the helium WD donor case, which is the scenario most relevant for Bildsten et al. (2007).

Rotation: Yoon & Langer (2004) found that rotation may be problematic for the initiation of a detonation in accreted helium shells. They found that the spin-up of the WD due to the accretion and resulting dissipation due to differential rotation might cause helium flashes to occur for lower shell masses, which may lead to inhibition of a detonation in turn resulting in fewer sub- M_{Ch} SNe. However, Piro & Bildsten (2004) found that the accreted material will be brought into co-rotation with the WD already at low depths within the helium shell, and so as noted in Bildsten et al. (2007) rotation should not play a significant role in the heating of the helium shell and subsequent helium-ignition.

5.4 The link between sub-Chandrasekhar SNe Ia and their progenitors

While it is useful to understand how the host galaxy environment influences the SN ejecta/observables, it is also fundamentally important to find a direct physical connection between the progenitor population and the observational characteristics of SNe Ia. For some time it has been known that brighter SNe Ia occur more frequently among young stellar populations (Hamuy et al. 1995). Could it be possible that sub- M_{Ch} SNe Ia arising from the (prompt) helium star channel are brighter than those from the double WD channel? This may be the case particularly considering Model A1, where the core mass of the exploding star for the helium star channel is on average slightly larger than for the double-WD channel (see Figure 7), and thus is likely to produce more ^{56}Ni . We also note that for both Model A1 and Model G1.5, $\sim 70\%$ of progenitors with delay times < 1 Gyr have CO WD masses $> 1.0 M_{\odot}$ (CO core masses $> 0.9 M_{\odot}$), while this fraction is only $\sim 45\text{--}50\%$ for progenitors with delay times > 3 Gyr. However there is no *strong* trend in our models which indicates that more massive WDs explode among younger populations. The majority of the sub- M_{Ch} binaries are double WDs, and the MS lifetime (ZAMS mass) of the primary star does not play a dominant role in setting the delay time.

Another point worth considering is that the helium star channel progenitors undergo two CE events on a relatively short time-scale compared to the time the stars spend as a post-MS detached binary. Thus these binary systems should be hotter and may be more readily detectable than their (colder, longer lived) double-WD counterparts. Since these helium star channel SNe in our models are expected to occur a few Myr after the last CE phase, the detection of such an explosion will probably not be inhibited by circumstellar matter from the companion. However, since these explosions involving helium stars are expected to be found among young stellar populations, they are likely to occur in regions of active star formation where their detection may be thwarted by the presence of dust and possibly circumstellar matter from nearby stellar systems. The binary progenitors of the helium WD channel on the other hand, although more abundant at most delay times, should be harder to detect as

most of their evolutionary time is spent during the detached double WD phase.

In the study of Krueger et al. (2010), a trend between the central density of the exploding Chandrasekhar mass WD and the total amount of ^{56}Ni produced in the explosion was found. Arguing that WDs which experience a longer cooling time (prior to the onset of mass transfer) will have a higher central density at time of ignition, they conclude that older WDs will produce less ^{56}Ni and will therefore be dimmer. While all of their models produce similar amounts of iron-group elements, the amount of ^{56}Ni is smaller for the exploding WDs of higher central density. The reason for this is that during the thermonuclear burning in the deflagration phase, faster neutronization occurs at higher densities, which leads to a higher production of stable (more neutron-rich) isotopes at the expense of production of ^{56}Ni . However, the findings of the Krueger et al. (2010) study do not apply to our sub- M_{Ch} models since they only consider exploding Chandrasekhar mass WDs which undergo a deflagration phase, whereas our CO WDs are assumed to undergo a detonation at lower densities, in which case neutronization is unimportant.

Thus far, we have only found (possibly) a weak correlation between the mass of the exploding WD and delay time, making it difficult to infer a connection between observed brightness (^{56}Ni synthesised in the explosion) and progenitor age. Nevertheless, if a connection between the age of the primary CO WD and the production of ^{56}Ni can be made in sub- M_{Ch} explosions such that dimmer SNe Ia occur among older populations, this would have very exciting consequences for our study.

5.5 Conclusion

Our standard model population synthesis indicates that there are potentially enough sub- M_{Ch} progenitors to account for the rates of SNe Ia. Nevertheless, much uncertainty still remains regarding the formation and evolution of close binary stars: mass transfer and accretion efficiencies, effects of rotation and magnetic fields, impact of metallicity on stellar winds and subsequent stellar and binary evolution, the common envelope phase, etc. Even given a large population of potential progenitors for sub- M_{Ch} explosions, there remain open questions about the explosion itself. Hydrodynamical studies have previously shown that sub- M_{Ch} WDs with an overlying helium shell can undergo a double-detonation which looks like a SN Ia, though the real answer as to what fraction of these systems lead to SNe Ia explosions depends on specific details. Most critically, under exactly which conditions does helium ignition occur, and how does the nucleosynthesis proceed?

The sub- M_{Ch} model is the first model which demonstrates a sufficient number of SNe Ia events to account for all, or at least some substantial fraction of, SNe Ia (Model A1), as well as *two distinct formation channels with their own characteristic DTD*: A prompt (< 500 Myr) helium star channel originating from binaries with more massive secondaries, and a more delayed (> 500 Myr) double WD channel originating from AM CVn-like progenitor binaries with lower mass. Whether some or all of the sub- M_{Ch} models explored in this work really lead to thermonuclear explosions

that look like normal (or some subclass of) SNe Ia is still a topic which requires further study.

ACKNOWLEDGMENTS

AJR would like to thank the organisers of the 2010 Workshop on Nuclear Astrophysics at Ringberg Castle, the organisers of the Workshop on Progenitors of SNe Ia at the Lorentz Center in Leiden, as well as the following people in general for helpful discussions: Brian Metzger, Ivo Seitenzahl, Lars Bildsten, Ken Shen, Thomas Janka, Bo Wang, Craig Heinke, Ed Van den Heuvel, Rüdiger Pakmor and Paolo Mazzali. Also, AJR thanks J. Grindlay and the ChaM-Plane group at the Harvard-Smithsonian Center for Astrophysics for use of computing resources, where the *StarTrack* simulations were performed.

REFERENCES

- Abdikamalov, E.B., Ott, C.D., Rezzolla, L., Dessart, L., Dimmelmeier, H. Marekt, A., Janka, H.-T. 2010, *PhRvD*, 81, 044012
- Belczynski, K., Kalogera, V., & Bulik, T. 2002, *ApJ*, 572, 407
- Belczynski, K., Bulik, T., & Ruiter, A. J. 2005, *ApJ*, 629, 915
- Belczynski, K., Kalogera, V., Rasio, F. A., Taam, R. E., Zezas, A., Bulik, T., Maccarone, T. J., & Ivanova, N. 2008, *ApJS*, 174, 223
- Bildsten, L., Shen, K. J., Weinberg, N. N., & Nelemans, G. 2007, *ApJL*, 662, L95
- Bogomazov, A. I., & Tutukov, A. V. 2009, *Astronomy Reports*, 53, 214
- Branch, D., Livio, M., Yungelson, L. R., Boffi, F. R., & Baron, E. 1995, *PASP*, 107, 1019
- Brandt, T. D., Tojeiro, R., Aubourg, É., Heavens, A., Jimenez, R., & Strauss, M. A. 2010, *AJ*, 140, 804
- Cappellaro, E., Evans, R., & Turatto, M. 1999, *A&A*, 351, 459
- Clayton, G. C., Geballe, T. R., Herwig, F., Fryer, C., & Asplund, M. 2007, *ApJ*, 662, 1220
- Darbha, S., Metzger, B. D., Quataert, E., Kasen, D., Nugent, P., & Thomas, R. 2010, *MNRAS*, 409, 846
- De Donder, E., & Vanbeveren, D. 2004, *New Astron. Reviews*, 48, 861
- de Kool, M. 1990, *ApJ*, 358, 189
- Dessart, L., Burrows, A., Ott, C. D., Livne, E., Yoon, S.-C., & Langer, N. 2006, *ApJ*, 644, 1063
- Dessart, L., Burrows, A., Livne, E., & Ott, C. D. 2007, *ApJ*, 669, 585
- Eldridge, J. J., & Stanway, E. R. 2009, *MNRAS*, 400, 1019
- Fink, M., Röpke, F. K., Hillebrandt, W., Seitenzahl, I. R., Sim, S. A., & Kromer, M. 2010, *A&A*, 514, A53
- Fryer, C., Benz, W., Herant, M., & Colgate, S. A. 1999, *ApJ*, 516, 892
- Fryer, C.L., Brown, P.J., Bufano, F., Dahl, J.A., Fontes, C.J., Frey, L.H., Holland, S.T., Hungerford, A.L., Immler, S., Mazzali, P., Milne, P.A., Scannapieco, E., Weinberg, N., Young, P.A., 2009, *ApJ*, 707, 193
- Greggio, L. 2010, *MNRAS*, 406, 22
- Gilfanov, M., & Bogdán, Á. 2010, *Nat*, 463, 924
- Guillochon, J., Dan, M., Ramirez-Ruiz, E., Rosswog, S. *ApJ*, 709, L64
- Hachisu, I., Kato, M., Nomoto, K., & Umeda, H. 1999, *ApJ*, 519, 314
- Hachisu, I., Kato, M., & Nomoto, K. 2008, *ApJ*, 679, 1390
- Hamuy, M., Phillips, M. M., Maza, J., Suntzeff, N. B., Schommer, R. A., & Aviles, R. 1995, *AJ*, 109, 1
- Han, Z., & Podsiadlowski, P. 2004, *MNRAS*, 350, 1301
- Hayden, B. T., et al. 2010, *ApJ*, 722, 1691
- Hoeflich, P., & Khokhlov, A. 1996, *ApJ*, 457, 500
- Hurley, J. R., Tout, C. A., & Pols, O. R. 2002, *MNRAS*, 329, 897
- Iben, I., Jr., & Tutukov, A. V. 1984, *ApJS*, 54, 335
- Iben, I., Jr., Nomoto, K., Tornambe, A., & Tutukov, A. V. 1987, *ApJ*, 317, 717
- Iben, I., Jr., & Tutukov, A. V. 1991, *ApJ*, 370, 615
- Ivanova, N., & Taam, R. E. 2004, *ApJ*, 601, 1058
- Kawai, Y., Saio, H., & Nomoto, K. 1987, *ApJ*, 315, 229
- Kato, M., & Hachisu, I. 1999, *ApJL*, 513, L41
- Kato, M., & Hachisu, I. 2004, *ApJL*, 613, L129
- Kenyon, S. J., Livio, M., Mikolajewska, J., & Tout, C. A. 1993, *ApJL*, 407, L81
- Kromer, M., & Sim, S. A. 2009, *MNRAS*, 398, 1809
- Kromer, M., Sim, S. A., Fink, M., Röpke, F. K., Seitenzahl, I. R., & Hillebrandt, W. 2010, *ApJ*, 719, 1067
- Krueger, B. K., Jackson, A. P., Townsley, D. M., Calder, A. C., Brown, E. F., & Timmes, F. X. 2010, *ApJL*, 719, L5
- Leonard, D. C. 2007, *ApJ*, 670, 1275
- Li, W., Chornock, R., Leaman, J., Filippenko, A. V., Poznanski, D., Wang, X., Ganeshalingam, M., & Mannucci, F. 2010, *arXiv:1006.4613* (2010a)
- Li, W., et al. 2010, *arXiv:1006.4612*
- Livne, E. 1990, *ApJL*, 354, L53
- Livne, E., & Arnett, D. 1995, *ApJ*, 389, 695
- Mannucci, F., Della Valle, M., & Panagia, N. 2006, *MNRAS*, 370, 773
- Maoz, D., & Badenes, C. 2010, *MNRAS*, 407, 1314
- Maoz, D., Sharon, K., & Gal-Yam, A. 2010, *ApJ*, 722, 1879 (2010a)
- Maoz, D., Mannucci, F., Li, W., Filippenko, A. V., Della Valle, M., & Panagia, N. 2010, *arXiv:1002.3056*, *MNRAS* accepted (2010b)
- Meng, X., & Yang, W. 2010, *ApJ*, 710, 1310
- Mennekens, N., Vanbeveren, D., De Greve, J. P., & De Donder, E. 2010, *A&A*, 515, A89
- Metzger, B. D., Piro, A. L., & Quataert, E. 2009, *MNRAS*, 396, 1659
- Meurs, E. J. A., & van den Heuvel, E. P. J. 1989, *A&A*, 226, 88
- Miyaji, S., Nomoto, K., Yokoi, K., & Sugimoto, D. 1980, *PASJ*, 32, 303
- Nelemans, G., Portegies Zwart, S. F., Verbunt, F., & Yungelson, L. R. 2001, *A&A*, 368, 939 (2001a)
- Nelemans, G., Yungelson, L. R., Portegies Zwart, S. F., & Verbunt, F. 2001, *A&A*, 365, 491 (2001b)
- Nelemans, G., & Tout, C. A. 2005, *MNRAS*, 356, 753
- Nelemans, G., Yungelson, L. R., van der Sluys, M. V., & Tout, C. A. 2010, *MNRAS*, 401, 1347
- Nomoto, K., & Kondo, Y. 1991, *ApJL*, 367, L19

- Nomoto, K., Saio, H., Kato, M., & Hachisu, I. 2007, *ApJ*, 663, 1269
- Nugent, P., Baron, E., Branch, D., Fisher, A., & Hauschildt, P. H. 1997, *ApJ*, 485, 812
- Pakmor, R., Kromer, M., Röpke, F. K., Sim, S. A., Ruiter, A. J., & Hillebrandt, W. 2010, *Nat*, 463, 61 (2010a)
- Pakmor, R., et al. 2010, in preparation. (2010b)
- Passey et al., 2010, in preparation.
- Piersanti, L., Cassisi, S., Iben, I., Jr., & Tornambé, A. 1999, *ApJL*, 521, L59
- Piersanti, L., Gagliardi, S., Iben, I., Jr., & Tornambé, A. 2003, *ApJ*, 598, 1229
- Piro, A. L., & Bildsten, L. 2004, *ApJ*, 610, 977
- Prialnik, D., & Kovetz, A. 1995, *ApJ*, 445, 789
- Pritchett, C. J., Howell, D. A., & Sullivan, M. 2008, *ApJL*, 683, L25
- Raskin, C., Scannapieco, E., Rhoads, J., & Della Valle, M. 2009, *ApJ*, 707, 74
- Regös, E., Tout, C. A., Wickramasinghe, D., Hurley, J. R., & Pols, O. R. 2003, *New Astron.*, 8, 283
- Roelofs, G. H. A., Nelemans, G., & Groot, P. J. 2007, *MNRAS*, 382, 685
- Ruiter, A. J., Belczynski, K., & Fryer, C. 2009, *ApJ*, 699, 2026 (Paper I)
- Ruiter, A. J., Belczynski, K., Benacquista, M., Larson, S. L., & Williams, G. 2010, *ApJ*, 717, 1006
- Saio, H., Nomoto, K. 1985, *A&A*, 150, L21
- Scannapieco, E., & Bildsten, L. 2005, *ApJL*, 629, L85
- Seitenzahl, I. R., Meakin, C. A., Townsley, D. M., Lamb, D. Q., & Truran, J. W. 2009, *ApJ*, 696, 515
- Shen, K. J., & Bildsten, L. 2007, *ApJ*, 660, 1444
- Shen, K. J., & Bildsten, L. 2009, *ApJ*, 699, 1365
- Shigeyama, T., Nomoto, K., Yamaoka, H., & Thielemann, F.-K. 1992, *ApJL*, 386, L13
- Sim, S. A., Röpke, F. K., Hillebrandt, W., Kromer, M., Pakmor, R., Fink, M., Ruiter, A. J., & Seitenzahl, I. R. 2010, *ApJL*, 714, L52
- Solheim, J.-E., & Yungelson, L. R. 2005, 14th European Workshop on White Dwarfs, 334, 387
- Taam, R. E. 1980, *ApJ*, 242, 749
- Totani, T., Morokuma, T., Oda, T., Doi, M., & Yasuda, N. 2008, *PASJ*, 60, 1327
- Tout, C. A., Regös, E., Wickramasinghe, D., Hurley, J. R., & Pols, O. R. 2001, *MSA*, 72, 371
- van der Sluys, M. V., Verbunt, F., & Pols, O. R. 2006, *A&A*, 460, 209
- van Kerkwijk, M. H., Chang, P., & Justham, S. 2010, *ApJL*, 722, L157
- Wang, B., Meng, X., Chen, X., & Han, Z. 2009, *MNRAS*, 395, 847 (2009a)
- Wang, B., Chen, X., Meng, X., & Han, Z. 2009, *ApJ*, 701, 1540 (2009b)
- Webbink, R. F. 1984, *ApJ*, 277, 355
- Whelan, J., & Iben, I. J. 1973, *ApJ*, 186, 1007
- Woosley, S. E., & Weaver, T. A. 1994, *ApJ*, 423, 371
- Yoon, S.-C., & Langer, N. 2003, *A&A*, 412, L53
- Yoon, S.-C., & Langer, N. 2004, *A&A*, 419, 645
- Yoon, S.-C., Podsiadlowski, P., & Rosswog, S. 2007, *MNRAS*, 380, 933
- Yungelson, L. R., Livio, M., Tutukov, A. V., & Saffer, R. A. 1994, *ApJ*, 420, 336
- Yungelson, L., Livio, M., Tutukov, A., & Kenyon, S. J. 1995, *ApJ*, 447, 656
- Yungelson, L., & Tutukov, A. 1997, *Stellar Ecology: Advances in Stellar Evolution*, 237
- Yungelson, L., & Livio, M. 1998, *ApJ*, 497, 168
- Yungelson, L. R., & Livio, M. 2000, *ApJ*, 528, 108
- Yungelson, L. R. 2008, *Astronomy Letters*, 34, 620
- Zorotovic, M., Schreiber, M. R., Gänsicke, B. T., & Nebot Gómez-Morán, A. 2010, *A&A*, 520, A86